

RECTANGULAR MICROSTRIP RESONATOR ILLUMINATED BY NORMAL-INCIDENT PLANE WAVE

M. Pergol* and W. Zieniutycz

Gdansk University of Technology, 11/12 Narutowicza Str., Gdansk-Wrzeszcz 80-233, Poland

Abstract—In the paper, an Illuminating Modes concept is introduced in order to find microstrip antenna parameters — resonant frequency, resonant resistance and radiation pattern. The concept is based on illuminating the rectangular patch by a single normally-incident plane wave. It results in the surface current density induced on the patch which is found by means of two-dimensional Spectral Domain Approach. Then, the resonant frequency, the quality factor, the resonant resistance and the radiation pattern of the analysed antenna are found. Application of Illuminating Mode concept in Spectral Domain Approach effects in analysis simplification and less time consuming calculations with no waste of the accuracy. Exemplary results for several kinds of radiators are presented, showing satisfactory level of agreement with published data.

1. INTRODUCTION

Microstrip antennas are widely used in various kinds of devices in almost every type of wireless and radar applications. From the theoretical point of view a single rectangular microstrip radiator can be treated as a lossy resonator of a quality factor related to the radiation phenomenon. There are a lot of theoretical and numerical tools [1–3] that enable to describe radiation from such a radiator and provide results useful in practical application [4]. The Spectral Domain Approach (SDA) is one of the most efficient tools, convenient and time saving on the stage of numerical implementation. In literature one can find two approaches of SDA: (i) one-dimensional [5–8] and (ii) two-dimensional [9, 10]. The first one is generally destined for analysis of transmission lines. However, if the field variation along

Received 29 June 2011, Accepted 24 August 2011, Scheduled 30 August 2011

* Corresponding author: Mariusz Pergol (mper@eti.pg.gda.pl).

one dimension is small enough, it can also be applied for analysis of the resonator. It takes place eg., for rectangular planar patch operating with fundamental mode TM_{01} . The results presented in [7] confirmed the utility of such an approach. Two-dimensional approach is oriented on solving the problems with 2D field variations. A complex frequency is introduced in order to find a nontrivial solution of characteristic Equations [9, 10] that permits then to find the surface current (more precisely the coefficients of the basis functions expansion used to approximate the surface current). Note that such an approach need no excitation. Therefore, some authors analyse resonators excited by a probe, what yields the current density, radiation pattern and input impedance [11].

In this paper, two-dimensional SDA is applied to analyse the radiation phenomena of rectangular microstrip radiator. We extended the concept of Hybrid Radiation Mode (HRM) and the condition at infinity for HRM of microstrip line [7] for two-dimensional case of a planar rectangular resonator. In order to describe the radiation phenomena the concept of so called Illuminating Mode (IM) is introduced. As a single IM we will call an elementary plane wave, illuminating the structure, the current induced on the patch and the scattered field.

In this method, the rectangular patch is illuminated by a single plane wave. A surface current density induced on the rectangular patch is found from SDA via method of moments. Then, the resonant frequency and radiation resistance are obtained from resonant curve of the surface current and equivalent capacitance of the patch. The radiation pattern is found with help of angular spectrum concept. Application of single IM to approach the radiation effect remarkably simplifies the solution with no waste of accuracy.

In the paper, SDA is employed to calculate a diffraction response of the obstacle (microstrip resonator) illuminated by an elementary plane wave. This method leads to find radiator parameters necessary in an antenna design. According to the best knowledge of the authors, diffraction theorem presented in literature (eg., [12–15]) is used rather to calculate radiation pattern or RCS for fixed structures, whereas design issue is often omitted.

Proposed IM can be extended for analysis of Frequency Selective Structures (FSS), in which excitation of normally incident plane wave is one of the most desired. Unlike the author, who introduced a vector spectral domain in order to illuminate the structure by plane wave [16], in this publication, we show how the normal incidence of plane wave can be implemented in SDA approach.

In Section 2, we introduce the concept of Illuminating Modes

and explain how the radiation field can be composed of such modes. Section 3 describes the implementation of the concept for the case of rectangular microstrip radiator. In particular we show that condition at infinity for Hybrid Radiation Mode in 2D case does not lead to iterative procedure as in the 1D case (i.e., transmission line problem). The exemplary calculations for rectangular radiator parameters (resonant frequency, radiation resistance, radiation pattern) compared to the results obtained from other approaches are also presented in this section. The last section of the paper is the conclusion.

2. THEOREM

Let us consider the structure shown in the Fig. 1. The rectangular patch of size $L \times W$ is located on the substrate of dielectric constant ϵ_r and thickness h . Both the substrate and the ground plane are infinite in the x and y directions. The lossless dielectric substrate is denoted as the 1st region and open lossless region as 2nd one. Note, that the patch is assumed to have negligible thickness compared to its width. The finite thickness can be analysed in SDA by treating the metallization as a separate layer [17], but it is neglected in our analysis. Let us define the Fourier transform of an electric and magnetic fields changing with the time (for convenience the coefficient $e^{i\omega t}$ is omitted):

$$\tilde{F}(k_x, k_y) = \iint F(x, y)e^{-i(k_x x + k_y y)} dx dy \tag{1}$$

where: $F = \{E, H\}$ are electric and magnetic field components, $\tilde{F} = \{\tilde{E}, \tilde{H}\}$ are their transforms.

Application of the transform (1) to the wave equation yields:

$$\nabla_z^2 \tilde{F}_{xi}(k_x, k_y, z) + k_{zi}^2 \tilde{F}_{xi}(k_x, k_y, z) = 0 \quad i = \{1, 2\} \tag{2}$$

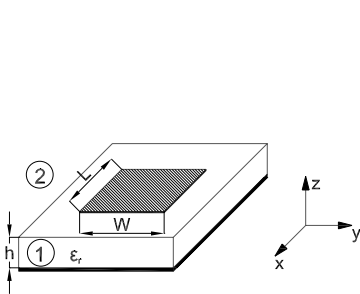


Figure 1. Rectangular microstrip radiator.

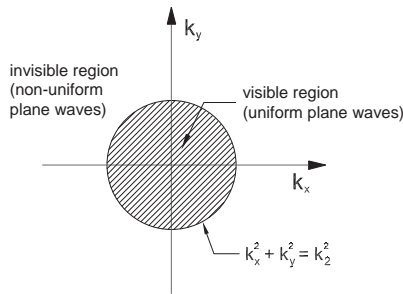


Figure 2. Visible and invisible regions of the (k_x, k_y) plane.

with well known form of the solution in open region:

$$\tilde{F}_{x2}(k_x, k_y, z) = A_{F2}(k_x, k_y)e^{+ik_{z2}z} + B_{F2}(k_x, k_y)e^{-ik_{z2}z} \quad (3)$$

where:

$$k_{z2} = \sqrt{k_2^2 - k_x^2 - k_y^2} = \sqrt{k_2^2 - \rho^2} \quad (4)$$

and $k_2 = \omega\sqrt{\epsilon_2\mu_2}$, $\rho^2 = k_x^2 + k_y^2$.

Note that wave Equation (2) involves only x -component of an electric (magnetic) field, that corresponds to resonant dimension of the structure.

Let us now discuss the radiation phenomena based on the analysis of spectral plane (k_x, k_y) shown in the Fig. 2. The spectral representation of the fields in open region consists of the continuum of uniform and non-uniform plane waves [18]. Wavenumber k_{z2} is purely imaginary in the invisible region and real in the visible one. As a consequence, if the structure excitation is to exist, the spectral representation of the field consists of both incoming $A_{F2}(k_x, k_y)e^{+ik_{z2}z}$ and outgoing $B_{F2}(k_x, k_y)e^{-ik_{z2}z}$ plane waves, so that the boundary condition at the interface $z = h$ is fulfilled. It has been shown [19] that in case of modes from visible part (incoming and outgoing waves) the radiation condition is fulfilled, if the eigenfunctions are bounded. Note, that taking into account only outgoing waves it results in no excitation.

2.1. Illuminating Modes Concept

Each point (k_{x0}, k_{y0}) inside the circle ($\rho < k_2$) corresponds to a particular direction (ϕ_0, θ_0) , from which the radiator is illuminated by an elementary plane wave of spectral representation $A_{E2}(k_{x0}, k_{y0})e^{+ik_{z20}z}$:

$$k_{x0} = k_2 \sin \theta_0 \cos \phi_0 \quad (5)$$

$$k_{y0} = k_2 \sin \theta_0 \sin \phi_0 \quad (6)$$

$$k_{z20} = \sqrt{k_2^2 - k_x^2 - k_y^2} \quad (7)$$

Point (k_{x0}, k_{y0}) is also related to the direction of an elementary reflected plane wave $(B_{E2}(k_{x0}, k_{y0})e^{-k_{z20}z})$. It means, that all points inside the circle form the continuum of the incoming and outgoing waves from all possible physical directions ($\theta \in \langle 0, \pi \rangle$, $\phi \in \langle 0, 2\pi \rangle$). Let us now assume that the structure is illuminated by a single plane wave, incoming from a given direction (ϕ_0, θ_0) . It results in reflected and scattered fields and also in a surface current induced on the patch. Both reflected and scattered fields depend on the direction

of incoming plane wave. The current induced on the patch is also a function of (ϕ_0, θ_0) . All physical phenomena (reflected field, scattered field and surface current) related to a single plane wave incoming from direction (ϕ_0, θ_0) will be called Illuminating Mode $IM(k_{x0}, k_{y0})$. The scattered field, necessary to calculate the radiation pattern, is a part of $IM(k_{x0}, k_{y0})$ and can be found in an analogous manner as induction theorem shows [20] — the current induced on the patch is a source of scattered field. Therefore, the scattered field is found by using the current distribution excited by incoming plane wave, but excluding the excitation.

It should be strongly emphasised, that both the current and the scattered field consist of the continuum of both parts of spectral plane: (i) inside the circle $(\rho < k_2)$, corresponding to far field, and (ii) outside the circle $(\rho \geq k_2)$, corresponding to near field. Thanks to this, the boundary conditions in $x0y$ plane for tangential field components at the interface $z = h$ are fulfilled.

To relate the unknown amplitudes of incoming and outgoing waves we can apply the condition at infinity for Hybrid Radiation Mode (described for 1D case in [7]). According to Equation (3) the electric and magnetic fields in the open region are expressed as:

$$\tilde{E}_{x2}(k_x, k_y, z) = A_{E2}(k_x, k_y)e^{+ik_{z2}z} + B_{E2}(k_x, k_y)e^{-ik_{z2}z} \quad (8)$$

$$\tilde{H}_{x2}(k_x, k_y, z) = A_{H2}(k_x, k_y)e^{+ik_{z2}z} + B_{H2}(k_x, k_y)e^{-ik_{z2}z} \quad (9)$$

From Maxwell equations we calculate the component $\tilde{E}_{y2}(k_x, k_y, z)$

$$\tilde{E}_{y2}(k_x, k_y, z) = -\frac{1}{k_2^2 - k_x^2} \left[k_x k_y \tilde{E}_{x2}(k_x, k_y, z) + -i\omega\mu k_{z2} \left(A_{H2}(k_x, k_y)e^{+ik_{z2}z} - B_{H2}(k_x, k_y)e^{-ik_{z2}z} \right) \right] \quad (10)$$

Let assume that the structure is shielded from top by electric wall at $z = D$. The components \tilde{E}_{x2} and \tilde{E}_{y2} are therefore the tangential components, so they should vanish even if this wall is moved to the infinity [19]. As a result this condition can be written in the following form:

$$\lim_{z \rightarrow \infty} \begin{bmatrix} A_{E2}(k_x, k_y) & B_{E2}(k_x, k_y) \\ \frac{i\omega\mu k_{z2}}{k_2^2 - k_x^2} A_{H2}(k_x, k_y) & \frac{-i\omega\mu k_{z2}}{k_2^2 - k_x^2} B_{H2}(k_x, k_y) \end{bmatrix} \begin{bmatrix} e^{+ik_{z2}z} \\ e^{-ik_{z2}z} \end{bmatrix} = \begin{bmatrix} 0 \\ 0 \end{bmatrix} \quad (11)$$

whose nontrivial solution is of the form:

$$A_{E2}(k_x, k_y)B_{H2}(k_x, k_y) + A_{H2}(k_x, k_y)B_{E2}(k_x, k_y) = 0 \quad (12)$$

and can be rewritten as:

$$A_{H2}(k_x, k_y) = \left(q_1 + q_2 \frac{\tilde{E}_y^h(k_x, k_y)}{\tilde{E}_x^h(k_x, k_y)} \right) \cdot A_{E2}(k_x, k_y) \quad (13)$$

where:

$$q_1 = \frac{k_x k_y}{\omega \mu_2 k_{z2}} \quad q_2 = \frac{k_2^2 - k_x^2}{\omega \mu_2 k_{z2}} \quad (14)$$

Note, that Equation (12) has the same form as condition at infinity for HRM [7]. However, it concerns resonant structures (2D), whereas HRM defined in [7] describes the radiation mode of waveguiding structures.

In the next step Equation (13) is applied to the classical formulation of SDA relating the currents and the fields at interface $z = h$ (see Fig. 1):

$$[G][\tilde{J}] = [\tilde{E}] + [\Delta][a] \quad (15)$$

where:

$[G]$ — dyadic Green's function,

$[\tilde{J}] = [\tilde{J}_x(k_x, k_y), \tilde{J}_y(k_x, k_y)]^T$ — vector of surface current densities on the patch,

$[\tilde{E}] = [\tilde{E}_x^h, \tilde{E}_y^h]^T$ — vector of electric fields at the plane $z = h$,

$[\Delta]$ — matrix of forcing amplitudes,

$$[a] = \begin{cases} [A_{E2}(k_x, k_y), A_{H2}(k_x, k_y)]^T & \text{for } \rho < k_2 \\ [0, 0]^T & \text{for } \rho \geq k_2 \end{cases}$$

The components of vector $[\tilde{J}]$ are expressed as the sum of basis functions $\tilde{j}_{xi}(k_x, k_y)$, $\tilde{j}_{yi}(k_x, k_y)$:

$$\tilde{J}_x(k_x, k_y) = \sum_{i=1}^{N_x} a_i \cdot \tilde{j}_{xi}(k_x, k_y) \quad \tilde{J}_y(k_x, k_y) = \sum_{i=1}^{N_y} b_i \cdot \tilde{j}_{yi}(k_x, k_y) \quad (16)$$

where N_x , N_y are the numbers of basis functions.

After applying Galerkin method over Equation (15), we obtained wanted basis coefficients a_i and b_i : Let remind, that excitation amplitudes $A_{E2}(k_x, k_y)$ and $A_{H2}(k_x, k_y)$ are related by Equation (13). Therefore, the problem can be solved using iterative procedure [7]. However, applying single Illumination Mode simplifies the calculations. It eliminates both iterative procedure and integration on the right side of Equation (15) as shown in the following subsection.

2.2. Normal Illuminating Mode

A single Illuminating Mode denoted as IM(0,0) corresponds to a normally incident, x -polarised plane wave. Spectral amplitudes related to IM(0,0) are therefore:

$$A_{E2}(k_x, k_y) = \delta(0,0) \quad A_{H2}(k_x, k_y) = 0 \quad (17)$$

It is worth to discuss the relation between these amplitudes as a function of illumination angle (see Equation (13)). For normal illumination we assume $k_x = k_y = 0$ and due to the fact that $\tilde{E}_y(k_x, k_y)$ is an odd function of k_x we have $A_{H2}(k_x, k_y) = 0$. In the case of illumination along axis k_x or k_y ($k_x \cdot k_y = 0$) the result will be equal ($A_{H2}(k_x, k_y) = 0$). For different illumination angles we can find the spectral amplitude $A_{H2}(k_x, k_y)$ directly from the relation (13), if $A_{E2}(k_x, k_y) = \delta(k_x, k_y)$ is assumed. Let remind that Dirac function $\delta(k_x, k_y)$ is a spectral representation of a single plane wave. Note, that the application of spectral amplitudes (17) eliminates the iterative procedure proposed in [7]. Moreover, due to Dirac Delta function features, integration occurred in the inner product containing the excitation function is vanished. It results in simplification of calculation and time saving. Thanks to application of Galerkin method obtained currents $\tilde{J}_x(k_x, k_y)$ and $\tilde{J}_y(k_x, k_y)$ fulfill the boundary condition at the interface $z = h$. As mentioned in previous subsection, the current transforms consist of two parts: inner ($\rho < k_2$) and outer ($\rho \geq k_2$) parts of circle $\rho^2 = k_2^2$. Therefore, the electric field (scattered field) at $z = h$ found from:

$$[\tilde{E}] = [G][\tilde{J}] \quad (18)$$

contains also both parts so it can be applied to calculate field in region 1:

$$\tilde{E}_{i1}(k_x, k_y, z) = \frac{\sin(k_{z1}z)}{\sin(k_{z1}h)} \tilde{E}_i(k_x, k_y, h), \quad 0 \leq z \leq h, \quad i = \{x, y\} \quad (19)$$

$$\tilde{E}_{z1}(k_x, k_y, z) = i \frac{k_{z1} \cos(k_{z1}z)}{k_{z2} \sin(k_{z1}h)} \tilde{E}_{z2}(k_x, k_y, h), \quad 0 \leq z \leq h, \quad (20)$$

and in region 2:

$$\tilde{E}_{i2}(k_x, k_y, z) = \tilde{E}_i(k_x, k_y, h) e^{-ik_{z2}(z-h)}, \quad z \geq h, \quad i = \{x, y\} \quad (21)$$

$$\tilde{E}_{z2}(k_x, k_y, z) = \tilde{E}_{z2}(k_x, k_y, h) e^{-ik_{z2}(z-h)}, \quad z \geq h, \quad (22)$$

where:

$$\tilde{E}_x(k_x, k_y, h) = G_{11}(k_x, k_y) \tilde{J}_x(k_x, k_y) + G_{12}(k_x, k_y) \tilde{J}_y(k_x, k_y) \quad (23)$$

$$\tilde{E}_y(k_x, k_y, h) = G_{21}(k_x, k_y) \tilde{J}_x(k_x, k_y) + G_{22}(k_x, k_y) \tilde{J}_y(k_x, k_y) \quad (24)$$

$$\tilde{E}_{z2}(k_x, k_y, h) = -\frac{k_x \tilde{E}_x(k_x, k_y, h) + k_y \tilde{E}_y(k_x, k_y, h)}{k_{z2}} \quad (25)$$

It should be noted that the relations above are valid in both visible and invisible regions. Therefore, knowledge of surface density current and electric field at $z = h$ permits us to calculate fundamental parameters of the antenna as shown in the following section.

3. NUMERICAL RESULTS

In the first part of this section we show how to calculate parameters of the patch antenna using the proposed method. In order to calculate the parameters of exemplary rectangular microstrip radiator, two dimensional SDA has been implemented in *Matlab* environment. The radiators are illuminated by $IM(0,0)$ corresponding to a normally-incident, x -polarised plane wave. All the fundamental parameters have been calculated and compared with data obtained from ADS Momentum simulator, which uses the method of moments. In the second part of this section the comparison of other patches is shown and some comments are added. As a basis and test functions the trigonometric ones are used with $N_x = 4$ and $N_y = 4$ for resonant and nonresonant directions, respectively.

3.1. Resonant Frequency

The structure that is analysed in this case study is a single patch located on the substrate of 0.79 mm height and of 2.22 electric permittivity. The length and the width of the radiator are equal to 25 mm and 40 mm, respectively. The resonant frequency is found from observation of the current of $IM(0,0)$. Sweeping over the interesting frequency range forms the resonance curve of the radiator current density (\tilde{J}_x). The frequency for which the maximum amplitude occurs is a resonance frequency (f_r). It should be noted that the resonant

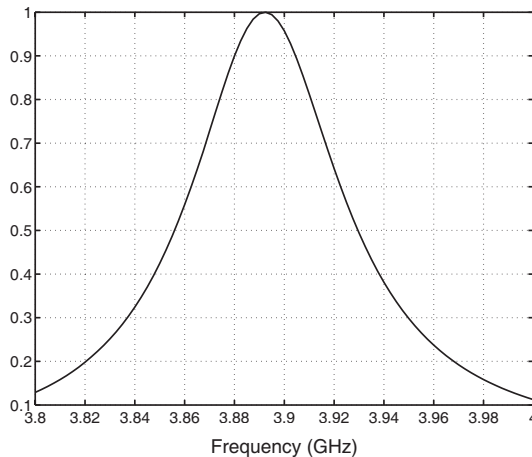


Figure 3. Normalized squared magnitude of surface current density ($|\tilde{J}_x(k_x, k_y)|^2$) induced on the patch by $IM(0,0)$ mode.

frequency is actually related to aniresonance, for which radiation resistance, corresponding to the radiation ability of the antenna, takes sufficiently large values. The resonance curve for the sum of squared magnitude of base coefficients a_i (see Equation (16)) for analysed structure is shown in Fig. 3. The maximal surface density current occurs at $f_r = 3.89$ GHz, whereas the frequency obtained from ADS Momentum equals 3.87 GHz. Note that the quality factor can be found in this curve and we will use it later to calculate the radiation resistance.

In the Fig. 4 the surface density current ($J_x(x, y)$) at resonant frequency is shown. It can be clearly seen that the most intensiveness

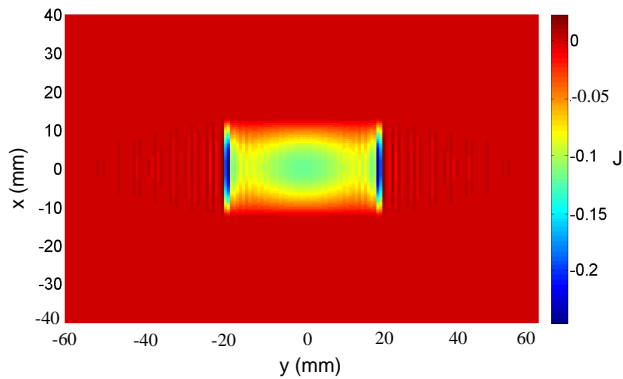


Figure 4. Surface current density ($J_x(x, y)$) induced on the patch by $IM(0, 0)$ mode.

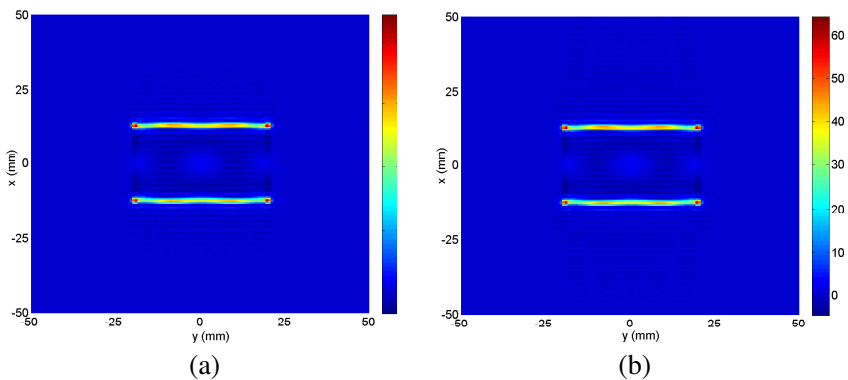


Figure 5. Resonant component of an electric field ($E_x(x, y)$) at $z = h$. (a) Real part. (b) Imaginary part.

of the current is focused on the edges. Some nonzero values occurred outside the patch are caused by a finite range of integration in the inverse Fourier transform.

The electric field on the $z = h$ plane is calculated in the next step using (18). The result is shown in Fig. 5. The maximum density of the electric field is focused in the close vicinity of the radiating edge as was expected.

3.2. Radiation Pattern

The radiation pattern can be expressed as a function of Fourier transforms of the fields components defined over the whole $x0y$ plane at $z = h$ [18]. In the first step we use the x and y components of electric field obtained from (18) to find the z the component:

$$\tilde{E}_z^h(k_x, k_y) = -\frac{k_x \tilde{E}_x^h(k_x, k_y) + k_y \tilde{E}_y^h(k_x, k_y)}{k_z} \quad (26)$$

Next, we find the asymptotic values ($z \rightarrow \infty$) of electric field components and we transform them to the spherical coordinate system. Note, that in the far field region the radial component of the field should be equal to zero so applying this property we can calculate the far field transversal components:

$$E_\theta(r, \theta, \phi) \sim \frac{ik_2 e^{-ik_2 r}}{2\pi r} \cos \theta \cdot \left[\tilde{E}_x^h(k_x, k_y) \cos \theta \cos \phi + \tilde{E}_y^h(k_x, k_y) \cos \theta \sin \phi - \tilde{E}_z^h(k_x, k_y) \sin \theta \right] \quad (27)$$

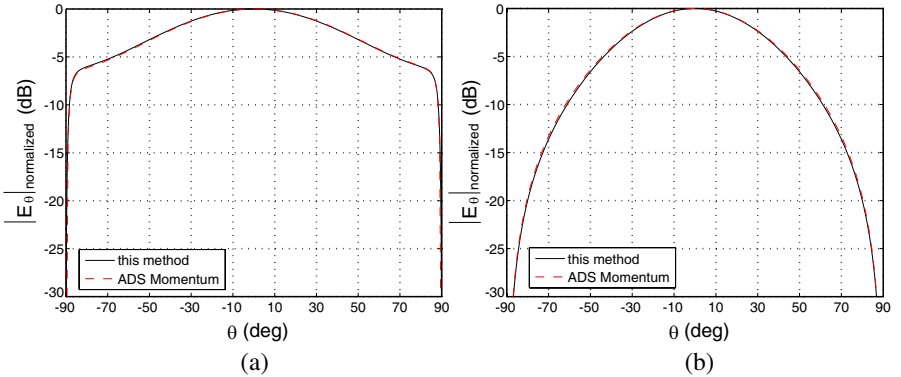


Figure 6. Radiation pattern of the antenna: (a) E -plane. (b) H -plane.

$$E_\phi(r, \theta, \phi) \sim \frac{ik_2}{2\pi} \frac{e^{-ik_2 r}}{r} \cos \theta \cdot \left[\tilde{E}_x^h(k_x, k_y) \sin \phi + \tilde{E}_y^h(k_x, k_y) \cos \phi \right] \quad (28)$$

where k_x and k_y are related to the the variables (θ, ϕ) by (5) and (6). After applying Equations (27) and (28) radiation pattern can be calculated.

The radiation patterns in two cuts, E -plane and H -plane are presented in Figs. 6(a) and 6(b), respectively. In the same Figure the patterns calculated by ADS Momentum are also presented. The both patterns are almost identical so it confirms the proper calculation of the electric field at $z = h$ plane.

3.3. Radiation Resistance

The radiation resistance is found from a cavity model. The quality factor (Q_{rad}) is distinguished from the resonance curve of the current (see Fig. 3 antenna) . Then the capacity of equivalence cavity (C_{ec}) is calculated [7]. All calculated variables are then substituted into:

$$R_{rad} = \frac{Q_{rad}}{2\pi f_r C_{ec}} \quad (29)$$

The calculated radiation resistance for analysed structure is equal to 180Ω , whereas the resonant resistance of the same patch fed by short (about 1% of the patch length) microstrip line, simulated in ADS Momentum equals 169Ω .

The presented results show a good accuracy of the presented method. Small differences in case of radiation resistance results from the estimation in cavity model.

3.4. Resonant Frequencies and Radiation Resistances of Different Patches

The comparison of 5 different rectangular microstrip antennas is shown in Tables 2 and 3. Dimension of radiators are shown in Table 1. Two parameters that are compared: resonant frequencies and radiation resistances. The results are obtained from ADS Momentum, from the proposed method (this method) and from one-dimensional SDA presented in [6, 7] (1D). Additionally the comparison of calculation time for proposed method and ADS Momentum is shown in Table 4. The standard mesh density ($\lambda/20$) has been applied for ADS Momentum calculation.

One can see that convergence of results is very accurate in terms of resonant frequencies. For a thin substrate the difference between 1D and 2D approaches is small enough. It can be easily explained as the

field variation along the nonresonant dimension is very small in this case. For structures with more significant thickness the results of the proposed method are close to results obtained from Momentum. It is clear that the assumption of no variation along nonresonant dimension is not fulfilled in this case.

The radiation resistance is more sensitive to the precision of the field calculation than the resonant frequency and this effect is observed in Table 3. The differences between proposed approach and results

Table 1. Dimension of analysed resonators.

name	W [mm]	L [mm]	h [mm]	ϵ_r
rct_01	40	25	0.79	2.22
rct_02	30	20	1.32	10.2
rct_03	40	25	1.59	2.22
rct_04	30	19	2.64	10.2
rct_05	29.5	19.5	3.07	2.33

Table 2. Resonant frequency [GHz] of different resonators.

name	this method	ADS Momentum	1D SDA [7]
rct_01	3.89	3.87	3.88
rct_02	2.28	2.27	2.27
rct_03	3.78	3.77	3.77
rct_04	2.30	2.29	2.27
rct_05	4.42	4.50	4.39

Table 3. Radiation resistance [Ω] of different resonators.

name	this method	ADS Momentum	1D SDA [7]
rct_01	180	167	111
rct_02	502	458	196
rct_03	191	174	122
rct_04	610	433	-
rct_05	278	204	-

Table 4. Normalised calculation time for single frequency point.

name	this method	ADS Momentum
rct_01	1.00	2.15
rct_02	1.00	2.00
rct_03	1.00	2.11
rct_04	1.00	2.11
rct_05	1.00	2.18

from Momentum are of order several percents for thin substrates and are much lower (about three times) than for 1D SDA. For a thick substrate even 2D approach leads to the results which cannot be acceptable. It means that another model (not cavity) should be applied in such a case. However, such types of the antennas are generally realised on thin substrates .

In terms of calculation time the proposed method is about two times more efficient than ADS Momentum (see Table 4).

4. CONCLUSION

In the paper the concept of Illuminating Modes has been introduced and implemented for the analysis of microstrip rectangular resonators by means of Spectral Domain Approach. The structure has been excited by a single Illuminating Mode $IM(0,0)$, corresponding to a normally incoming plane wave. It has been shown that a single mode excitation is sufficient enough to induce a surface current on the patch, which, in turn, is a source of a complete spectrum of the antenna fields (near and far field). Choice of a single Illuminating Mode $IM(0,0)$ to excite the structure also results in the significant simplification of the calculation — the computation time is about two times shorter compared to ADS Momentum for standard mesh density ($\lambda/20$). Proposed analysis can be used to find the antenna parameters. Resonant frequency, radiation pattern and radiation resistance have been calculated using the proposed method. Good agreement with results obtained from the full wave simulator has been achieved. Therefore, the method can be applied to antenna arrays or different shapes of patches under the condition of changes in basis function. It is worth to mention, that the method can be potentially applied for analysing of FSS, for which a normal incident plane wave is one of the most desired excitations.

ACKNOWLEDGMENT

This work was supported in part by the system project “Innodoktorant-Scholarships for Ph.D. students, III edition” (project co financed by the European Union in the frame of the European Social Fund) and in part by the Polish Ministry of Science and Higher Education from sources for science under COST Action IC0603, decision No 478/N-COST/2009/0.

REFERENCES

1. Takahashi, M., T. Arima, and T. Uno., “FDTD analysis of printed antenna on thin dielectric sheet including quasi-static approximation,” *IEEE Antennas and Propagation Society International Symposium*, Vol. 1, 1022–1025, 2004.
2. Li, L. W., S. Gao, and A. Sambell, “FDTD analysis of a dual-frequency microstrip patch antenna,” *Progress In Electromagnetics Research*, Vol. 54, 155–178, 2005.
3. He, S., Y. Chen, S. Yang, and Z. Nie. “Fast analysis of microstrip antennas over a frequency band using an accurate mom matrix interpolation technique,” *Progress In Electromagnetics Research*, Vol. 109, 301–324, 2010.
4. Bahl, I., R. Garg, P. Bhartia, and A. Ittipiboon, *Microstrip Antenna Design Handbook*, Artech House, Boston, London, 2000.
5. Mrkvice, J., J. Zehentner, and J. Machac, “Spectral domain analysis of open planar transmission lines,” *Microwave Review*, Vol. 10, No. 2, 36–42, 2004.
6. Zieniutycz, W., “Application of hybrid radiation modes of a microstrip line in the design of rectangular microstrip antennas,” *IEE Proceedings — Microwaves, Antennas and Propagation*, Vol. 145, No. 5, 421–423, October 1998.
7. Zieniutycz, W., “Hybrid radiation modes of microwave integrated circuit (MIC) lines-theory and application,” *Progress In Electromagnetics Research*, Vol. 56, 299–322, 2006.
8. Marynowski, W., P. Kowalczyk, and J. Mazur, “On the characteristic impedance definition in microstrip and coplanar lines,” *Progress In Electromagnetics Research*, Vol. 110, 219–235, 2010.
9. Itoh, T. and W. Menzel, “A full-wave analysis method for open microstrip structures,” *IEEE Transactions on Antennas and Propagation*, Vol. 30, No. 6, 1191–1196, November 1982.

10. Kataria, N., A. Kedar, and K. Gupta, "Spectral-domain modeling of superconducting microstrip structures: transmission lines and resonators," *Microwave and Optical Technology Letters*, Vol. 41, No. 1, 55–59, April 2004.
11. Pozar, D., "Input impedance and mutual coupling of rectangular microstrip antennas," *Electronics Letters*, Vol. 29, No. 1, 63–68, January 1981.
12. Wu, Z.-S. and J.-J. Zhang, "Composite electromagnetic scattering from the plate target above a one-dimensional sea surface: taking the diffraction into account," *Progress In Electromagnetics Research*, Vol. 92, 317–331, 2009.
13. Apostol, M. and G. Vaman, "Plasmons and diffraction of an electro-magnetic plane wave by a metallic sphere," *Progress In Electromagnetics Research*, Vol. 98, 97–118, 2009.
14. Hong, T., L.-T. Jang, Y.-X. Xu, S.-X. Gong, and W. Jiang, "Radiation and scattering analysis of a novel circularly polarized slot antenna," *Journal of Electromagnetic Waves and Applications*, Vol. 24, No. 13, 1709–1720, 2010.
15. Eom, H. J., *Electromagnetic Wave Theory for Boundary-Value Problems*, Springer, Berlin, Heidelberg, 2004.
16. Qing, A., "Vector spectral-domain method for the analysis of frequency selective surfaces," *Progress In Electromagnetics Research*, Vol. 65, 201–232, 2006.
17. Jansen, R. H., "The spectral-domain approach for microwave integrated circuits," *IEEE Transactions on Microwave Theory and Techniques*, Vol. 33, No. 10, 1043–1056, October 1985.
18. Rhodes, D. R., *Synthesis of Planar Antenna Sources*, Clarendon Press, Oxford, 1974.
19. Shevchenko, V. V., *Continuous Transitions in Open Waveguides*, Prentice Hall, Englewood Cliffs, NJ, 1973.
20. Harrington, R. R., *Time-Harmonic Electromagnetic Fields*, McGraw-Hill Book Company, New York, Toronto, London, 1961.